

# Crystal Structure and Spectroscopic Properties of the CT Complex of Methyl Viologen Dication and *o*-Dimethoxybenzene Included in a Polycyano–Polycadmuate Host and Electrostatic Effects on Its CT Absorption

Hirofumi Yoshikawa and Shin-ichi Nishikiori\*

Department of Basic Science, Graduate School of Arts and Sciences, The University of Tokyo, 3-8-1, Komaba, Meguro, Tokyo 153-8902, Japan

Toshimasa Ishida

Molecular Clusters Division, Research Center for Molecular-Scale Nanoscience, Institute for Molecular Science, Okazaki National Research Institutes, Okazaki 444-8585, Japan

Received: April 17, 2003; In Final Form: June 13, 2003

Using the polycyano–polycadmuate host that is a negative-charged Cd cyanide complex with a framework structure built with  $\text{Cd}^{2+}$  ions and bridging cyanide ligands, we synthesized a clathrate including methyl viologen dication ( $\text{MV}^{2+}$ ) and *o*-dimethoxybenzene (ODMB) as guests. The color of the clathrate was reddish-brown, and its origin was considered to be a charge transfer (CT) interaction of a CT complex formed with  $\text{MV}^{2+}$  as an acceptor and ODMB as a donor in the host. The wavelength at the CT absorption maximum was largely red shifted as compared with that of the CT complex in an acetonitrile solution. The single-crystal X-ray diffraction analysis revealed a  $\pi$ – $\pi$  stacking structure of the CT complex and a one-dimensional arrangement of the CT complexes in a channel-like cavity of the framework host. In the array of the CT complexes,  $\text{MV}^{2+}$  ions are adjacent to each other and their separation is short. The direction of the transition moment of the CT absorption determined from the structural information and the spectrum measured on a crystalline sample agreed with that derived from *ab initio* calculations at the CIS/6-31+G\* level. Our calculations also showed that the red shift of the CT absorption is mainly due to electrostatic effects between the CT complexes, not due to the shortening of the distance between  $\text{MV}^{2+}$  and ODMB, which is generally believed to be the reason. The negative-charged host stabilizes the ground state of the CT complex, but the electrostatic interaction between the CT complexes heightens the ground state and lowers the excited state. In this clathrate, due to the CT complex array with the short separation, the effect from the guests overcomes that from the host, and the red shift appears.

## Introduction

The polycyano–polycadmuate host clathrate<sup>1</sup> is a clathrate that had derived from the Hofmann type clathrate<sup>2</sup>. The host of the Hofmann type clathrate is made up with the character of a cyanide ligand as a bridging ligand. Similarly, the polycyano–polycadmuate host is a framework constructed with  $\text{Cd}^{2+}$  ions and cyanide ligands linking two  $\text{Cd}^{2+}$  ions. The  $\text{Cd}^{2+}$  ion has a tetrahedral, a trigonal bipyramidal, or an octahedral coordinating structure so that the polycyano–polycadmuate host has a large number of structural variations. Although many studies have been carried out on the polycyano–polycadmuate host clathrate, their aims have been the structural development for extending its multidimensional host structure and its inclusion capability, and no study for developing functionalized materials by use of the host has been found. Under these circumstances, we tried to synthesize a new polycyano–polycadmuate host clathrate with chemical or physical properties by the combination of the polycyano–polycadmuate host and methyl viologen dication ( $\text{MV}^{2+}$ , 1,1'-dimethyl-4,4'-bipyridinium dication) that is known as a strong electron acceptor.<sup>3,4</sup> In general, the polycyano–polycadmuate host clathrate consists of three parts: (i) a negative-

charged host of a Cd–cyanide complex with a framework structure; (ii) a cationic guest to neutralize the negative charge of the host, such as  $\text{N}(\text{CH}_3)_4^+$ ,  $\text{S}(\text{CH}_3)_3^+$ ,  $\text{NH}_2(\text{CH}_2)_3\text{NH}(\text{CH}_3)_2^+$ , etc.; and (iii) an ordinary organic molecule guest that is termed a neutral guest. The two kinds of guests are trapped in the framework host. Our attempt was to use  $\text{MV}^{2+}$  as a cationic guest and to include it into the framework host together with an arene donor as a neutral guest. In such a clathrate, electronic interactions among the host and the two kinds of guests are expected. The clathrates obtained in our preparative studies were classified into two groups.<sup>5,6</sup> The clathrates in the first group, whose arene guests had relatively high ionization potentials, were colorless but turned blue on irradiation of UV light. This photoinduced color change comes from the photo-reduction from  $\text{MV}^{2+}$  to  $\text{MV}^{+\bullet}$ , and its details were reported in our previous paper.<sup>5</sup> The clathrates in the second group had their own color by nature. The ionization potentials of their arene guests were lower than those of the first group. The origin of the color was considered to come from the charge transfer (CT) interaction of a CT complex formed with  $\text{MV}^{2+}$  and the arene donor in the host,<sup>6</sup> and this scheme was computationally confirmed.<sup>7</sup> In this paper, we concentrate our attention on the color of the clathrates of the second group and carry out a more detailed investigation.

\* To whom correspondence should be addressed. Tel and Fax: +81 3 5454 6569. E-mail: cnskor@mail.ecc.u-tokyo.ac.jp.

We here pick up a clathrate including  $MV^{2+}$  and *o*-dimethoxybenzene (ODMB) as a typical case and confirm the formation of a CT complex of  $MV^{2+}$  and ODMB in the polycyano–polycadmate host and its CT interaction using the single-crystal X-ray structure determination, spectroscopic measurements on the clathrate in a powdered and a crystalline state, and *ab initio* calculations. In the course of the spectroscopic measurements, it was found that the wavelength at the CT absorption maximum of the CT complex in the clathrate was largely red shifted as compared with that in an acetonitrile solution. We examine two factors for this red shift by simulating spectra. One is an effect of the shortening of the donor–acceptor distance. This shortening is generally considered as a reason for lowering the excitation energy of a CT complex. In the case of a CT complex in a clathrate, the inclusion of a CT complex into a host makes its donor–acceptor distance short so that the red shift arises. However, this scheme cannot hold in our case. The other factor is an electrostatic effect coming from the host and the guests surrounding the CT complex. This effect resembles the solvent effect in a sense. Our calculations show the importance of this effect for the CT absorption in this clathrate. Using the information of the crystal structure obtained here, the electrostatic effect from the surroundings is discussed in detail.

As a recent trend in chemistry, the development of functionalized materials and molecules with interesting chemical or physical properties is actively carried out by use of an assembly of plural components based on the concept of supramolecular chemistry. The combination of  $MV^{2+}$  and a solid state matrix is an attempt in this line. Several examples of the CT complex of  $MV^{2+}$  confined in a solid state matrix have been known, and there are some discussions on their properties.<sup>8–10</sup> However, in many cases, they are given with no structural information. Our spectroscopic experiments and theoretical calculations have been carried out on the basis of the structural information obtained by the single-crystal X-ray determination. In this regard, we believe that our results bring more reliable information on the understanding of these kinds of systems.

## Experimental Section

**Preparation.** The  $MV^{2+}$ –ODMB clathrate was prepared by a method similar to that described in our previous paper.<sup>5</sup>  $K_2[Cd(CN)_4]$  (5 mmol, 1.47 g),  $CdCl_2 \cdot 2.5H_2O$  (5 mmol, 1.14 g), and  $MVCl_2$  (methyl viologen dichloride, 2 mmol, 0.50 g) were dissolved in water (50 mL). After the solution was filtered, ODMB was poured into the filtrate, and then the mixture was stored at room temperature. The clathrate was obtained as reddish-brown needlelike crystals after a few days. Anal. calcd for  $[MV^{2+}][Cd_3(CN)_{6.553}Cl_{1.447}(H_2O)] \cdot C_6H_4(OCH_3)_2$ ,  $(C_{26.553}H_{26}N_{8.553}O_3Cl_{1.447}Cd_3)$ : C, 35.38; H, 2.91; N, 13.29. Found: C, 35.5; H, 2.88; N, 13.5%. The nonstoichiometric formula, which was determined by the X-ray structure determination demonstrated in the next section, comes from a structural disorder of the host complex.

**Crystal Structure Determination.** X-ray diffraction intensity data of a single crystal of the clathrate, which was coated with epoxy resin to prevent liberation of ODMB, were collected using a Rigaku R-Axis RAPID imaging plate diffractometer with graphite monochromatized Mo  $K\alpha$  radiation ( $\lambda = 0.71069$  Å) at room temperature. Crystal data for  $[MV^{2+}][Cd_3(CN)_{6.553}Cl_{1.447}(H_2O)] \cdot C_6H_4(OCH_3)_2$ :  $C_{26.553}H_{26}N_{8.553}O_3Cl_{1.447}Cd_3$ ,  $FW = 901.47$ , orthorhombic, *Pnma* (no. 62),  $a = 15.4750(2)$  Å,  $b = 8.8408(1)$  Å,  $c = 25.0585(4)$  Å,  $U = 3428.29(8)$  Å<sup>3</sup>,  $Z = 4$ ,  $D_x = 1.746$  g cm<sup>−3</sup>,  $\mu(Mo K\alpha) = 1.98$  mm<sup>−1</sup>. The empirical

absorption correction<sup>11</sup> was applied to 51 929 reflections measured in the scan range of 2.64 and 59.88° in  $2\theta$ , and 5259 independent reflections ( $R_{int} = 0.053$ ) were used for the analysis. The positions of  $Cd^{2+}$  ions were determined by the direct method using the SHELXS-97 program.<sup>12</sup> The crystal structure was refined by the successive difference Fourier syntheses and full-matrix least-squares procedure using the SHELXL-97 program.<sup>13</sup> Anisotropic thermal factors were applied to all nonhydrogen atoms. Hydrogen atoms were introduced at positions geometrically calculated but were not included in the refinement. The refinement was carried out on  $F^2$ . The final reliability factors were  $R1(F) = 0.0324$  for reflections with  $I > 2\sigma(I)$ ,  $wR2(F^2) = 0.1075$ , and  $S = 0.881$  for all reflections and 228 parameters.<sup>14</sup> The maximum and minimum electron density residues found in the final differential Fourier syntheses were +0.578 and −0.844 eÅ<sup>−3</sup>, respectively.

**UV–Vis Spectra Measurements.** UV–vis absorption spectra of a  $[MV^{2+}][PF_6^-]_2$  and an ODMB acetonitrile solution were recorded on a JASCO V-570 UV–vis spectrometer. Crystals of the clathrate were washed with ethanol and acetone, dried, and then powdered. The powder was diluted with  $BaSO_4$  powder and packed into a flat cylindrical cell JASCO PSH-001 with a quartz window, and its diffuse reflectance spectrum was measured on a JASCO V-570 UV–vis spectrometer equipped with an ISN integrating sphere accessory. Absorption spectra of a single crystal of the clathrate, whose size was 1.8 mm × 0.2 mm × 0.1 mm, were recorded on an Olympus BX60 polarizing microscope attached with a JASCO CT-25C spectrophotometer and a Hamamatsu photoelectron multiplier R316 detector. The orientation of the single crystal was confirmed by the X-ray diffraction method.

**Theoretical Calculations.** In the modeling of molecular structures for theoretical calculations, the atomic coordinates determined in the above X-ray analysis were used. All molecular orbital (MO) calculations were performed on the  $MV^{2+}$ –ODMB guest pair by the Hartree–Fock (HF) method using the 6-31+G\* basis set, and excited states and vertical electronic transitions were treated by the configuration interaction with singles (CIS).<sup>15,16</sup> The solvent effect of an acetonitrile solution was calculated using the polarizable continuum model (PCM).<sup>17,7</sup> For the estimation of the electric charges on the atoms of the CT complex and the host to make a background charge distribution, the Merz–Kollman–Singh method at the MP2/6-31+G\* level and the charge equilibration method (QEq) were used. The Merz–Kollman–Singh method produces atomic charges based on an electrostatic potential,<sup>18</sup> and this method at the MP2/6-31+G\* level would be one of the most appropriate ways for our purpose. The Merz–Kollman–Singh method was used in the case of the CT complex. However, it was not realistic to apply the same method to the host because of the enormous CPU time. We applied the QEq method for obtaining the atomic charges of the host. The QEq method predicts charge distributions in various kinds of molecules based on geometry and experimental atomic properties.<sup>19</sup> All calculations were carried out using the Gaussian 98 program<sup>20</sup> on the SGI Origin 2800 workstation cluster systems at the Research Center for Computational Science, Okazaki National Research Institute. Excitation energies calculated are listed in Table 1.

## Results and Discussion

**Crystal Structure.** The host of the clathrate is a Cd complex with a two-dimensional (2D) network structure formed with cyanide ligands working as bridging ligands. The host Cd complex,  $[Cd_3(CN)_{6.553}Cl_{1.447}(H_2O)]^{2-}$ , contains three indepen-

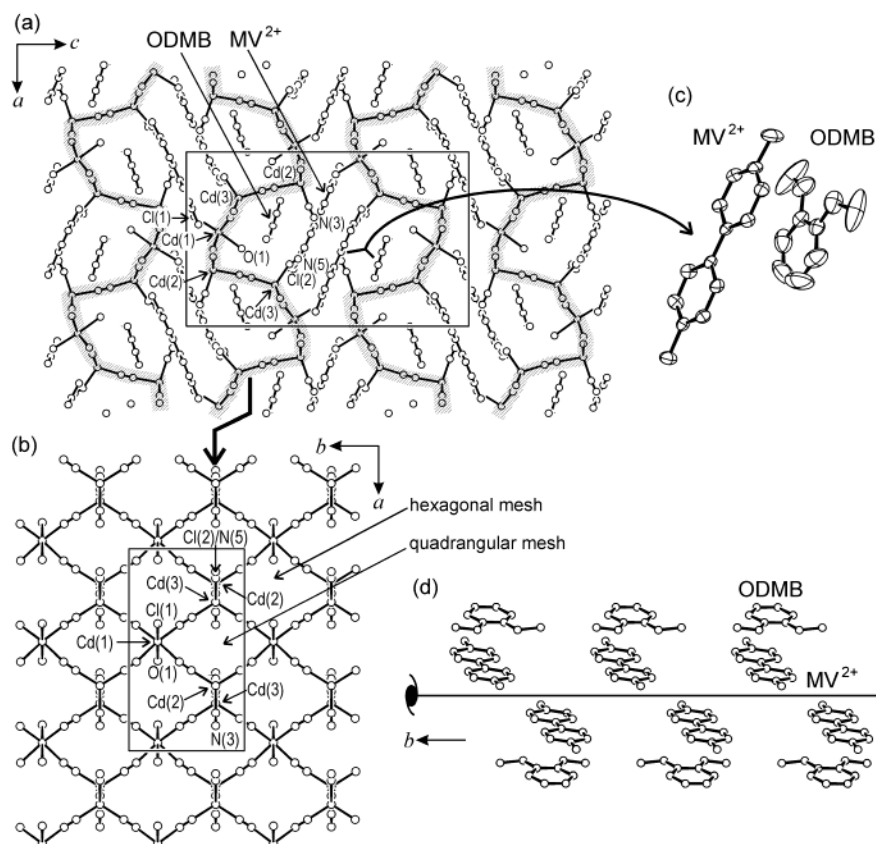


**Figure 1.** (a) Crystal structure of the clathrate viewed along the *b*-axis. Each gray thick line indicates the cross-section of the wavy 2D network host complex. The 1D channel-like cavity runs along the direction of the *b*-axis at the center of the unit cell. (b) A projective view of the 2D network host complex along the *c*-axis. The network consists of hexagonal and quadrangular meshes. (c) A perspective view of the  $MV^{2+}$ –ODMB CT complex in the clathrate. (d) The 1D arrangement of the CT complexes in the channel-like cavity. The complexes are related with a 2-fold screw axis parallel to the *b*-axis.

**TABLE 1: Excitation Energy ( $E_{CT}$ ) of the  $MV^{2+}$ –ODMB CT Complex**

	$E_{CT}$ (eV)
experimental values <sup>a</sup>	
the clathrate	2.55
the acetonitrile solution	3.44
calculated values <sup>b</sup>	
in vacuo	3.47
in an acetonitrile solution	4.28
in $3 \times 3 \times 3$ unit cells	
including host and guests	2.91
including only host	3.84
including only guests	2.51
in 3 CT complex array	
model 1	2.05
model 2	5.12

<sup>a</sup> Obtained from the diffuse reflectance and the absorption spectrum in Figure 2. <sup>b</sup> Calculated at the CIS/6-31+G\* level.

dent  $Cd^{2+}$  ions, which are located on a mirror plane perpendicular to the *b*-axis of the crystal. Cd(1) has an octahedral structure coordinated by a chloride ion Cl(1), a water molecule, and four cyanide ligands. Cd(2) has a distorted tetrahedral structure, whose shape is close to a trigonal pyramid, coordinated by four cyanide ligands. Cd(3) has a tetracoordinated structure, but a structural disorder was found at a coordinating site of Cd(3). At the site, a chloride ligand Cl(2) or a cyanide ligand C(5)–N(5) are coordinating randomly. Their occupancy factors were determined to be 0.447(4) for Cl(2) and 0.553(4) for C(5)–N(5) by the refinement calculations. This kind of disorder was sometimes observed in polycyano–polycadmate hosts.<sup>1f</sup> At the

other sites of Cd(3), three cyanide ligands are coordinating with no structural disorder. There are five independent cyanides in the crystal. Among them, three ligands work as a bridging ligand to make a bridge between  $Cd^{2+}$  ions, and a cyanide ligand at Cd(2) and the disordered cyanide ligand at Cd(3) act as a unidentate ligand. The basic structure of the host Cd complex is a 2D network formed with the bridging cyanide ligands. The 2D network spreads over a plane parallel to the *ab* plane of the crystal. However, its network plane is largely waved because of a glide plane *a* perpendicular to the *c*-axis, as shown in Figure 1a. The network consists of two kinds of meshes as illustrated in Figure 1b. One is a hexagonal mesh formed with the cyanide linkage of  $-Cd(1)-NC-Cd(3)-CN-Cd(2)-CN-Cd(1)-NC-Cd(2)-NC-Cd(3)-CN-$ , and the other is a quadrangular mesh formed with the linkage of  $-Cd(1)-NC-Cd(3)-CN-Cd(1)-NC-Cd(2)-CN-$ . The hexagonal mesh has a chair form structure, which resembles the chair form of a cyclohexane molecule. Its nonplanar structure generates the wavy 2D network structure. The whole structure of the crystal is a layered structure of the 2D networks stacked along the *c*-axis. The 2D networks are related with an inversion center of the crystal, so that the folds of the adjacent wavy 2D networks face each other and vacant space is generated there. This space works as a channel-like cavity, which extends one-dimensionally along the direction of the *b*-axis. At the center of the unit cell in Figure 1a, the cross-section of the channel-like cavity is seen. The unidentate ligands, the water molecule at Cd(1), the cyanide ligand at Cd(2), and the disordered chloride ion Cl(2) and cyanide ligand C(5)–N(5) at Cd(3), protrude from the surface of the 2D network to the inside of the channel-like cavity.



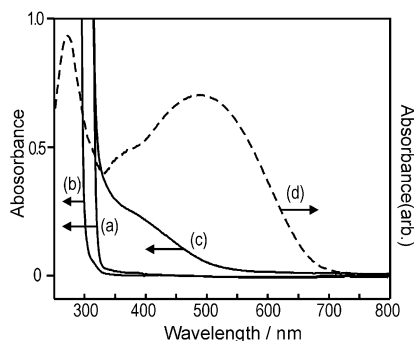


**Figure 2.** UV-vis absorption spectra: (a) a 0.03 M  $[\text{MV}^{2+}][\text{PF}_6^-]_2$  acetonitrile solution, (b) a 0.075 M ODMB acetonitrile solution, (c) an acetonitrile solution containing  $[\text{MV}^{2+}][\text{PF}_6^-]_2$  (0.03 M) and ODMB (0.03 M), and (d) diffuse reflectance spectrum of the clathrate.

In the channel-like cavity,  $\text{MV}^{2+}$  and ODMB are trapped as a guest pair whose structure is face-to-face stacking of one  $\text{MV}^{2+}$  ion and one ODMB molecule as shown in Figure 1a,c. As confirmed later, this guest pair is a CT complex. The dihedral angle of the two pyridinium rings of  $\text{MV}^{2+}$  about the central C—C bond was  $0^\circ$ . The molecular planes of  $\text{MV}^{2+}$  and ODMB are almost parallel to each other, and their interplane distance was  $3.49(1) \text{ \AA}$ . This stacking structure is usually observed in CT complexes formed between  $\text{MV}^{2+}$  and an arene donor.<sup>4,21</sup> As compared with known structural data of  $\text{MV}^{2+}$ , no abnormal bond length and angle were found in the  $\text{MV}^{2+}$  ion. In the channel-like cavity, the CT complexes are arranged one-dimensionally along the running direction of the cavity, but the stacking of the CT complexes does not exist because the molecular planes of  $\text{MV}^{2+}$  and ODMB are perpendicular to the *ac* plane and the CT complexes are related with a 2-fold screw axis running along the *b*-axis at the center of the channel-like cavity. Figure 1d shows this arrangement of the CT complexes in the channel-like cavity. In this CT complex array,  $\text{MV}^{2+}$  ions are adjacent to each other. The nearest distance between  $\text{MV}^{2+}$  ions was  $3.152 \text{ \AA}$  ( $\text{H}(102)\cdots\text{H}(106)^i$ ; *i*,  $-x, -y, -z$ ), and the distance between the molecular centers of the adjacent  $\text{MV}^{2+}$  ions was  $5.990 \text{ \AA}$ .

The distance between the oxygen atoms of ODMB and the water molecule at Cd(1) was  $2.85(1) \text{ \AA}$  ( $\text{O}(1)\cdots\text{O}(201)^{ii}$ ; *ii*,  $-x + 1/2, -y - 1, z + 1/2$ ). This distance indicates hydrogen bonding between the CT complex and the 2D network host. The N ends of the unidentate cyanide ligands and the Cl(2) chloride ligand are located near the reverse side of the  $\text{MV}^{2+}$  molecular plane facing ODMB. The distances between the  $\text{MV}^{2+}$  molecular plane and the ligands were  $3.45(1) \text{ \AA}$  for N(3)<sup>iii</sup> (*iii*,  $x - 1/2, -y + 1/2, -z + 1/2$ ),  $3.23(3) \text{ \AA}$  for N(5), and  $3.39(1) \text{ \AA}$  for Cl(2).

**CT Interaction.** The CT interaction of the  $\text{MV}^{2+}$ —ODMB guest pair trapped in the clathrate was confirmed from spectra of the clathrate in a powdered and a single crystalline state. Figure 2 shows the absorption spectra of a  $[\text{MV}^{2+}][\text{PF}_6^-]_2$  and an ODMB acetonitrile solution and a mixture of both. A new absorption band, which was not observed in each spectrum of the solution, was found at ca.  $360 \text{ nm}$  ( $3.44 \text{ eV}$ ) in the spectrum of the mixture. This new band is a CT absorption band of a CT complex of  $\text{MV}^{2+}$  and ODMB. In Figure 2, the diffuse reflectance spectrum of the clathrate is also shown, and its absorption maximum was found at  $486 \text{ nm}$  ( $2.55 \text{ eV}$ ). This absorption maximum was largely red shifted as compared with that found in the solution. To confirm that this absorption comes from the CT interaction of the  $\text{MV}^{2+}$ —ODMB pair trapped in the clathrate, some experiments were carried out using a single crystal of the clathrate and polarized light.<sup>22</sup>

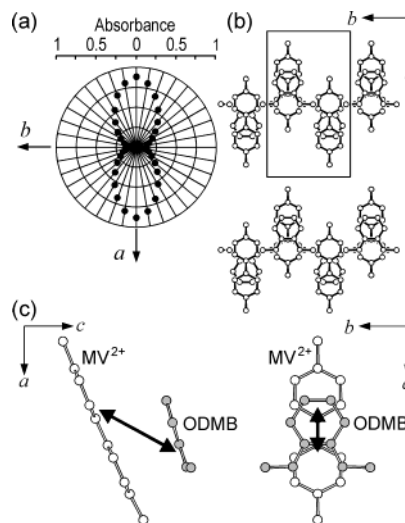


**Figure 3.** (a) Polar plots of the absorbance for the clathrate measured at  $550 \text{ nm}$  in the single crystalline phase. (b) Packing diagram of the  $\text{MV}^{2+}$ —ODMB guest pairs viewed on the *ab* plane. (c) The direction of the transition moment calculated at the CIS/6-31+G\* level for the transition with the lowest excitation energy of the  $\text{MV}^{2+}$ —ODMB guest pair. A projection along the *b*-axis (left) and that along the *c*-axis (right).

On the *ab* plane of a single crystal of the clathrate, dichroism was observed (Figure 1S in the Supporting Information). When the plane of polarized incident light, which was white light, was perpendicular to the *a*-axis of the crystal, the crystal was colorless. When the plane was parallel to the *a*-axis, the color of the crystal was reddish-brown. This observation indicates that the transition moment causing the reddish-brown color is parallel to the *a*-axis on the *ab* plane of the crystal. To determine its exact direction, the absorbance of the crystal was measured changing the angle between the *a*-axis of the crystal and the plane of polarized light from  $0$  to  $180^\circ$  every  $10^\circ$ . Used wavelength of the polarized incident light was  $550 \text{ nm}$ , which is a wavelength on the shoulder of the absorption band, because the absorbance at the absorption maximum was too large and quantitative measurement was not possible on our instrument. Figure 3a,b shows the polar plots of the absorbance obtained in the measurement and the packing diagram of the guest pairs in the clathrate, respectively. The polar plots indicate that the direction of the transition moment is exactly parallel to the *a*-axis on the *ab* plane. The measurements on the other faces of the crystal were not possible because the other faces were too narrow for the measurements.

The largest CI expansion coefficient for the lowest excited state derived from our calculation on the  $\text{MV}^{2+}$ —ODMB guest pair at the CIS/6-31+G\* level was  $0.70$ , and its excitation was from a state, whose main character is regarded as the highest occupied molecular orbital of ODMB, to a state that is regarded as the lowest unoccupied molecular orbital of  $\text{MV}^{2+}$  (Figure 2S in Supporting Information). The other CI expansion coefficients were less than  $0.1$ , and their contributions to this excitation are small. Therefore, the calculated excitation is concluded to be a CT transition from ODMB (donor) to  $\text{MV}^{2+}$  (acceptor). The calculation showed that its transition moment was running from ODMB to  $\text{MV}^{2+}$  as shown in Figure 3c. This direction corresponds to the direction of the *a*-axis on the *ab* plane of the crystal and also agrees with that of the transition moment observed. The results obtained from the calculations support that the  $\text{MV}^{2+}$ —ODMB guest pair in the clathrate is a CT complex and the reddish-brown color observed comes from its CT interaction. The excitation energy calculated here was  $3.47 \text{ eV}$  and is higher than the observed value of  $2.55 \text{ eV}$ . This

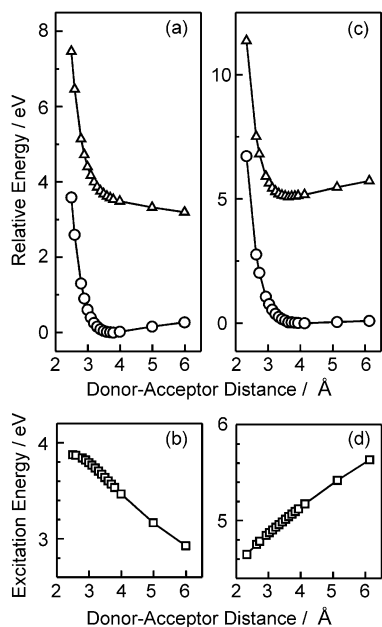


**Figure 4.** Potential energy curves for the ground state (open circle) and the excited state (open triangle) vs the donor–acceptor distance (top two graphs) and the plots of the excitation energy vs the donor–acceptor distance (bottom two graphs). The ground and excited states were calculated at the HF and CIS level using the 6-31+G\* basis set. (a,b) The MV<sup>2+</sup>–ODMB complex; (c,d) the naphthalene–tetracyanobenzene complex.

discrepancy is partly due to overestimation of the excitation energy in the CIS calculation.<sup>7</sup> However, it should be noted that our calculation at this stage does not include effects from the clathrate structure.

#### Effect of Shortening of the Donor–Acceptor Distance.

Although CT interaction of the MV<sup>2+</sup>–ODMB guest pair was confirmed above, the large red shift of the CT absorption remained as a problem. As a cause for such red shift of CT absorption, an effect of the shortening of the intermolecular distance between a donor and an acceptor is well-known. The differences in the minimum and the slope of the potential energy curves for the ground and the excited state of a CT complex are the essential reason.<sup>23</sup> Similar phenomena including red shift and blue shift were reported in MV<sup>2+</sup>–arene donor CT complexes confined in a zeolite matrix.<sup>9,10</sup> In the case of the red shift in a zeolite matrix, it was suggested that the shortening of the donor–acceptor distance, which arises from inclusion of a CT complex into a zeolite framework, generates the red shift.<sup>9</sup> In this study, first we examined this effect.

Calculations at the CIS/6-31+G\* level were performed on the MV<sup>2+</sup>–ODMB CT complex varying the donor (ODMB)–acceptor (MV<sup>2+</sup>) distance. The plots of the calculated potential energy curves of both states vs the donor–acceptor distance are shown in Figure 4a, and its excitation energies are plotted in Figure 4b. Although the curve for the ground state had a shallow minimum at 3.79 Å, that for the excited state showed a gradual decrease with an increase in the donor–acceptor distance and had no minimum. The excitation energy increased with a decrease in the donor–acceptor distance. This finding is opposite to the general trend mentioned before. To clarify this reason, we carried out the same calculation on a CT complex formed with naphthalene (donor) and tetracyanobenzene (acceptor), which is a noncharged CT complex. The geometrical data were cited from its crystal structure report.<sup>24</sup> Its energy curves and excitation energy are shown in Figure 4c,d, respectively. In this case, the excitation energy decreased with

a decrease in the donor–acceptor distance and the potential curves for the ground and the excited state had minimum values at 4.13 and 3.63 Å, respectively. These results agree with the general trend. The difference between both cases is in their electric charges. Needless to say, the MV<sup>2+</sup>–ODMB CT complex is a dication. In the excited state, where an electron is transferred from ODMB to MV<sup>2+</sup>, its charge distribution is described as MV<sup>+</sup>–ODMB<sup>+</sup>. This charge distribution causes electrostatic repulsion between both components, and this repulsion is larger with decreasing the donor–acceptor distance.<sup>25</sup> On the other hand, in the case of the naphthalene–tetracyanobenzene CT complex, the charge distribution in the excited state is described as naphthalene<sup>+</sup>–tetracyanobenzene<sup>−</sup>. An attractive force works between them, and the system becomes more stable with decreasing the donor–acceptor distance. These situations are seen on the energy curves for their excited states in Figure 4a,c and cause the aspects opposite to each other shown in Figure 4b,d. Our calculations have clarified that the shortening of the donor–acceptor distance cannot be a reason for the red shift of the CT absorption in the MV<sup>2+</sup>–ODMB CT complex.

**Electrostatic Effect from the Surroundings.** Next, we investigated electrostatic effects coming from the surroundings, which means the host and the guest pairs. Thus, we carried out a CIS/6-31+G\* calculation on one CT complex that is surrounded by the electric charges of the atoms in the host and the other CT complexes. The electric charges were located as point charges at the atomic positions determined in the X-ray work and were included in the CIS calculation as a background charge distribution. The spatial range including the CIS calculation was that of 3 × 3 × 3 unit cells, which is the smallest range surrounding a one unit cell at the center. The charges on the atoms of the CT complex were obtained by the Merz–Kollman–Singh method<sup>18</sup> at the MP2/6-31+G\* level. The atomic charges calculated for H atoms of MV<sup>2+</sup> were in the range between −0.16 and +0.26 and those for O atoms of ODMB were ca. −0.48. The total charge on MV<sup>2+</sup> was +1.87, and the percentage of CT from ODMB to MV<sup>2+</sup> was 0.065, which is in a previously reported range of 0.02 and 0.074.<sup>26</sup> The charges of the host were calculated by the QEq method.<sup>19,27</sup> The structural disorder of the host was treated by adding together two charge sets calculated for the host with full Cl(2) and that with full C(5)–N(5) using their occupancy factors as weight. All atomic charges and coordinates included in the calculation are listed in tables in the Supporting Information.

The excitation energy calculated by this CIS calculation was 2.91 eV, which is larger than the experimental value of 2.55 eV due to overestimation of the excitation energy in the CIS calculation. However, this calculated value is smaller than those of 3.47 and 4.28 eV, which were calculated as the excitation energy in the gas phase and that in an acetonitrile solution, respectively. These values indicate that the red shift was reproduced by the calculation. To analyze this result in detail, we divided the calculation into two parts, the contribution from the host and that from the guests.

To estimate the effect from only the host, the same calculation was performed including the electric charges on the atoms of the host, and a value of 3.84 eV was obtained for the excitation energy. As compared with the value for the gas phase of 3.47 eV, this result means that the inclusion by the host gives rise to blue shift of CT absorption. This blue shift resembles the blue shift sometimes observed in a polar solvent solution.<sup>29</sup> As shown in the previous section, the polarity of the MV<sup>2+</sup>–ODMB CT complex is greater in the ground state than in the excited state,

which may be described as  $MV^+-ODMB^+$ . As a result, the energy of the ground state is lowered more than that of the excited state by electrostatic interaction between the CT complex and the polar solvent molecules, and the blue shift appears in a solution. Considering the structural situation of the CT complex in our clathrate, where the CT complex is held by the framework host with negative charges, and the situation in a solution of a polar solvent, where the CT complex is surrounded by oriented polar solvent molecules, it is reasonable that the host and a polar solvent cause a similar effect on CT absorption. In a solution, however, polar solvent molecules can reorient and take the most suitable arrangement for lowering the energy of the system, while in the host such the rearrangement of the atomic charges is impossible. This is considered to be the reason that the blue shift in the host is smaller than that in an acetonitrile solution.

The same calculation carried out including only atomic charges of the CT complexes surrounding the central CT complex gave a small value of 2.51 eV for the excitation energy. It is clear that the red shift is originated in the electrostatic effect from the guests. As an origin of this red shift, we considered an electrostatic interaction shown in the following. In the channel-like cavity of this clathrate, the  $MV^{2+}$ –ODMB complexes are related with the 2-fold screw axis and are arranged one-dimensionally as shown in Figure 1d. In this arrangement,  $MV^{2+}$  ions are adjacent to each other and their separation is short. In this structural situation, the CT complex in the ground state is instable because of the electrostatic repulsion between  $MV^{2+}$  ions. However, in the excited state, where its electric charge distribution changes to  $MV^+-ODMB^+$ , the instability coming from the repulsion between  $MV^{2+}$  ions is relaxed. This instable ground state and relaxed excited state bring the red shift of the excitation energy. To confirm this idea, we carried out similar calculations including atomic charges of a small CT complex array consisting of three CT complexes. In this time, two models were made. One model (model 1) had the arrangement of  $MV^{2+}$  and ODMB as found in the clathrate, which is shown in Figure 1d. In the other model (model 2), the positions of  $MV^{2+}$  and ODMB were exchanged without destroying the basic arrangement made by the 2-fold screw axis, so that the nearest intermolecular distance is the separation between adjacent ODMB molecules and  $MV^{2+}$  ions that are sufficiently separated. If the electrostatic interaction takes large part in the red shift, the excitation energy in model 2 becomes larger because of its lowered ground state and heightened excited state. The calculated values were 2.05 and 5.12 eV for model 1 and model 2, respectively. These results ascertain the electrostatic effect to be an origin of the red shift.

The molecular arrangement of the CT complexes found in the host is peculiar to our clathrate. In many cases, the arrangement seen in a CT complex of  $MV^{2+}$  and an arene donor is an array of alternate  $MV^{2+}$  and arene with face-to-face stacking. In the case of ODMB, this general trend was confirmed from the crystal structure of a simple CT complex of  $[MV^{2+}][PF_6^-]_2[ODMB]$ , which was prepared from an aqueous solution containing  $[MV^{2+}][PF_6^-]_2$  and ODMB.<sup>30</sup>  $MV^{2+}$  and ODMB are alternately arrayed and make a column, where their  $\pi$  planes are face-to-face stacked. Among these columns, the counteranions of  $PF_6^-$  are located. The color of the crystal was yellow, and its CT absorption maximum was measured at 410 nm in its diffuse reflectance spectrum. No large red shift as found in the clathrate was observed. The arrangement of the  $MV^{2+}$ –ODMB CT complexes in the clathrate is clearly unfavorable in the sense of the electrostatic interaction. The negative charged host and its structure surrounding the positive

charged CT complexes are considered to stabilize the arrangement of the CT complexes. Therefore, the red shift observed here is characteristic of this clathrate.

## Conclusions

In the  $MV^{2+}$ –ODMB guest pair trapped in the polycyano–polycadmate host of  $[Cd_3(CN)_{6.553}Cl_{1.447}(H_2O)]^{2-}$ , the formation of a CT complex and CT transition was confirmed by the crystal structure determination, spectroscopic measurements, and theoretical calculations. The observed large red shift of the CT absorption comes not from the shortening of the donor–acceptor distance due to the inclusion by the host but from the electrostatic interaction between adjacent CT complexes in the channel-like cavity of the host. These findings indicate the importance of the electrostatic effect from the surroundings in a clathrate compound similarly to that in a solution. The difference between both states is their structural flexibility. In the case of a clathrate, the positions of electric charges surrounding the CT complex are fixed and their spatial arrangement depends on the structure of the host. Our results suggest a possibility of controlling spectroscopic properties of a CT complex by the design of a host structure.

The one-dimensional (1D) array of  $MV^{2+}$  ions found in this clathrate arouses interest from a different viewpoint. Recently, several papers that described details of a complex formed with an arene cation and its parent arene have been published.<sup>31</sup> The complex can be regarded as a mixed valence dimer. In the 1D array of  $MV^{2+}$  ions that can be partly reduced,  $MV^{2+}$  ion and its reduced one have a potential for having such a type of interaction, and in that case, interesting physical properties such as conductivity are expected.

As reported in our previous paper, there were more newly synthesized polycyano–polycadmate host clathrates including  $MV^{2+}$  and an arene donor.<sup>6</sup> They showed their own colors as observed in this clathrate. Probably, they have properties similar to this clathrate. The details on their crystal structures and spectroscopic and other physical properties will be reported elsewhere.

**Acknowledgment.** This work was supported by the Joint Studies Program (2002, project code by7) of the Institute for Molecular Science and by a Grant-in-Aid for Scientific Research (A) Project No. 12354008 and (C) Project No. 12640492 from the Japan Society for the Promotion of Science. We thank the Research Center for Computational Science, Okazaki National Research Institutes, for the use of the SGI Origin 2800 workstation and Prof. Nobuyuki Matsushita of The University of Tokyo for his technical support in the measurement of the single-crystal absorption spectra.

**Supporting Information Available:** CIF files for  $[MV^{2+}][Cd_3(CN)_{6.553}Cl_{1.447}(H_2O)] \cdot C_6H_4(OCH_3)_2$  and  $[MV^{2+}][PF_6^-]_2 \cdot [C_6H_4(OCH_3)_2]$ , pictures of the dichroism observed on the *ab* plane of the clathrate crystal and main molecular orbitals concerned in the CT transition, and tables of the atomic coordinates and charges used in the CIS/6-31+G\* calculations. This material is available free of charge via the Internet at <http://pubs.acs.org>.

## References and Notes

- (1) (a) Iwamoto, T. *Inclusion Compounds*; Atwood, J. L., Davis, J. E., D., MacNicol, D. D., Eds.; Oxford University Press: Oxford, 1991; Vol. 5, Chapter 6, p 177. (b) Iwamoto, T. *Comprehensive Supramolecular Chemistry*; MacNicol, D. D., Toda, F., Bishop, R., Eds.; Pergamon: Oxford, 1996; Vol. 6, Chapter 19, p 643. (c) Iwamoto, T. *J. Inclusion Phenom.*



- 1996, 24, 61. (d) Kitazawa, T.; Nishikiori, S.; Kuroda, R.; Iwamoto, T. *Chem. Lett.* **1988**, 459. (e) Kitazawa, T.; Nishikiori, S.; Kuroda, R.; Iwamoto, T. *Chem. Lett.* **1988**, 1729. (f) Kitazawa, T.; Nishikiori, S.; Iwamoto, T. *Mater. Sci. Forum* **1992**, 91–93, 257. (g) Nishikiori, S.; Ratcliffe, C. I.; Ripmeester, J. A. *J. Am. Chem. Soc.* **1992**, 114, 8590. (h) Kitazawa, T.; Nishikiori, S.; Iwamoto, T. *J. Chem. Soc., Dalton Trans.* **1994**, 3695. (i) Iwamoto, T.; Nishikiori, S.; Kitazawa, T. *Supramol. Chem.* **1995**, 6, 179.
- (2) Iwamoto, T. *Inclusion Compounds*; Atwood, J. L., Davis, J. E. D., MacNicol, D. D., Eds.; Academic Press: London, 1984; Vol. 1, Chapter 2, p 29.
- (3) (a) Bird, C. L. *Chem. Soc. Rev.* **1981**, 10, 49. (b) Śliwa, W.; Bachowska, B.; Zelichowicz, N. *Heterocycles* **1991**, 32, 2241 and references therein.
- (4) Monk, P. M. S. *The Viologens: Physicochemical Properties, Synthesis and Applications of the Salts of 4,4'-Bipyridine*; John Wiley & Sons: Chichester, 1998, and references therein.
- (5) (a) Yoshikawa, H.; Nishikiori, S. *Chem. Lett.* **2000**, 142. (b) Yoshikawa, H.; Nishikiori, S.; Watanabe, T.; Ishida, T.; Watanabe, G.; Murakami, M.; Suwinska, K.; Luboradzki, R.; Lipkowski, J. *J. Chem. Soc., Dalton Trans.* **2002**, 1907.
- (6) Yoshikawa, H.; Nishikiori, S.; Suwinska, K.; Luboradzki, R.; Lipkowski, J. *Chem. Commun.* **2001**, 1398.
- (7) Ishida, T.; Murakami, M.; Watanabe, G.; Yoshikawa, H.; Nishikiori, S. *Internet Electron. J. Mol. Des.* **2003**, 2, 14; <http://www.biochempress.com>.
- (8) (a) Yoon, K. B.; Kochi, J. K. *J. Am. Chem. Soc.* **1989**, 111, 1128. (b) Yoon, K. B.; Kochi, J. K. *J. Phys. Chem.* **1991**, 95, 3780. (c) Yoon, K. B. *Chem. Rev.* **1993**, 93, 321. (d) Yoon, K. B.; Hubig, S. M.; Kochi, J. K. *J. Phys. Chem.* **1994**, 98, 3865. (e) Hashimoto, S. *Tetrahedron* **2000**, 56, 6957. (f) Nanasawa, M.; Kaneko, M.; Kamogawa, H. *Bull. Chem. Soc. Jpn.* **1993**, 66, 1764. (g) Kim, H.-J.; Heo, J.; Jeon, W. S.; Lee, E.; Kim, J.; Sakamoto, S.; Yamaguchi, K.; Kim, K. *Angew. Chem., Int. Ed. Engl.* **2001**, 40, 1526.
- (9) (a) Yoon, K. B.; Huh, T. J.; Corbin, D. R.; Kochi, J. K. *J. Phys. Chem.* **1993**, 97, 6492. (b) Yoon, K. B.; Huh, T. J.; Kochi, J. K. *J. Phys. Chem.* **1995**, 99, 7042.
- (10) Park, Y. S.; Um, S. Y.; Yoon, K. B. *J. Am. Chem. Soc.* **1999**, 121, 3193.
- (11) *PROCESS-AUTO*. Automatic Data Acquisition and Processing Package for Imaging Plate Diffractometer; Rigaku Corporation: Tokyo, Japan, 1998.
- (12) Sheldrick, G. M. *SHELXS-97: Program for Crystal Structure Solution*; University of Göttingen: Germany, 1997.
- (13) Sheldrick, G. M. *SHELXL-97: Program for Crystal Structure Refinement*; University of Göttingen: Germany, 1997.
- (14) The reliability factors are defined as follows:  $R1 = \sum ||F_o| - |F_c|| / \sum |F_o|$ ,  $wR2 = \{ \sum [w(F_o^2 - F_c^2)^2] / \sum [w(F_o^2)^2] \}^{1/2}$ ; the weighting scheme was  $w = 1 / [\sigma^2(F_o^2) + (g_1 P)^2]$  where  $g_1 = 0.0513$  and  $P = [2F_c^2 + F_o^2] / 3$ ; the goodness of fit was  $S = \{ \sum [w(F_o^2 - F_c^2)^2] / (n - p) \}^{1/2}$  where  $n$  is the number of used reflections and  $p$  is the number of parameters. Crystallographic data were deposited in the Cambridge Crystallographic Data Center as CCDC 207321.
- (15) In our previous study, we calculated excited states of a  $MV^{2+}$ -mesitylene CT complex at the TDDFT B3LYP/6-31G\*\* and the CIS/6-31G\*\* level and obtained better results with the CIS calculation than the TDDFT B3LYP method.<sup>7</sup> Considering this experience and an economy of CPU time, we here used the CIS treatment.
- (16) See, for example, Jensen, F. *Introduction to Computational Chemistry*; John Wiley & Sons Ltd.: Chichester, 1999.
- (17) (a) Miertus, S.; Scrocco, E.; Tomasi, J. *Chem. Phys.* **1981**, 55, 117. (b) Miertus, S.; Tomasi, J. *Chem. Phys.* **1982**, 65, 239. (c) Cossi, M.; Barone, V.; Cammi, R.; Tomasi, J. *Chem. Phys. Lett.* **1996**, 255, 327.
- (18) (a) Besler, B. H.; Merz, K. M., Jr.; Kollman, P. A. *J. Comput. Chem.* **1990**, 11, 431. (b) Singh, U. C.; Kollman, P. A. *J. Comput. Chem.* **1984**, 5, 129.
- (19) Rappé, A. K.; Goddard, W. A. III. *J. Phys. Chem.* **1991**, 95, 3358.
- (20) Frisch, M. J.; Trucks, G. W.; Schlegel, H. B.; Scuseria, G. E.; Robb, M. A.; Cheeseman, J. R.; Zakrzewski, V. G.; Montgomery, J. A., Jr.; Stratmann, R. E.; Burant, J. C.; Dapprich, S.; Millam, J. M.; Daniels, A. D.; Kudin, K. N.; Strain, M. C.; Farkas, O.; Tomasi, J.; Barone, V.; Cossi, M.; Cammi, R.; Mennucci, B.; Pomelli, C.; Adamo, C.; Clifford, S.; Ochterski, J.; Petersson, G. A.; Ayala, P. Y.; Cui, Q.; Morokuma, K.; Malick, D. K.; Rabuck, A. D.; Raghavachari, K.; Foresman, J. B.; Cioslowski, J.; Ortiz, J. V.; Stefanov, B. B.; Liu, G.; Liashenko, A.; Piskorz, P.; Komaromi, I.; Gomperts, R.; Martin, R. L.; Fox, D. J.; Keith, T.; Al-Laham, M. A.; Peng, C. Y.; Nanayakkara, A.; Gonzalez, C.; Challacombe, M.; Gill, P. M. W.; Johnson, B. G.; Chen, W.; Wong, M. W.; Andres, J. L.; Head-Gordon, M.; Replogle, E. S.; Pople, J. A. *Gaussian 98*, revision A.11.1; Gaussian, Inc.: Pittsburgh, PA, 1998.
- (21) (a) Mulliken, R. S.; Person, W. B. *Annu. Rev. Phys. Chem.* **1962**, 13, 107. (b) Prout, C. K.; Wright, J. D. *Angew. Chem., Int. Ed. Engl.* **1968**, 7, 659. (c) Soos, Z. G. *Annu. Rev. Phys. Chem.* **1974**, 25, 121.
- (22) In the diffuse reflectance spectrum in Figure 2, another absorption band was recognized at ca. 375 nm. However, the assignment of this band by the calculation was not achieved because the direction of its transition moment could not be determined due to limitations of our instruments. Therefore, this band is not taken up as a subject for discussion in this paper.
- (23) (a) Tanaka, J.; Yoshihara, K. *Bull. Chem. Soc. Jpn.* **1965**, 38, 739. (b) Prochorow, J. *J. Chem. Phys.* **1965**, 43, 3394. (c) Prochorow, J.; Tramer, A. *J. Chem. Phys.* **1966**, 44, 4545. (d) Offen, H. W.; Studebaker, J. F. *J. Chem. Phys.* **1967**, 47, 253.
- (24) Kumakura, S.; Iwasaki, F.; Saito, Y. *Bull. Chem. Soc. Jpn.* **1967**, 40, 1826.
- (25) (a) Matos, M. S.; Gehlen, M. H. *Spectrochim. Acta Part A* **1998**, 54, 1857. (b) Matos, M. S.; Gehlen, M. H.; Trsic, M. *J. Mol. Struct. (Theochem.)* **1999**, 488, 233.
- (26) Murthy, A. S. N.; Bhardwaj, A. P. *Spectrochim. Acta Part A* **1982**, 38, 207.
- (27) Before performing the ab initio calculations, we examined the reliability of the QEq method using model compounds of  $[Cd(CN)_4]^{2-}$  and  $[Cd_2(CN)_7]^{3-}$ , which are primitive units of the polycyano-polycadmiate host.<sup>28</sup> The results obtained by the QEq method agreed substantially with those obtained by the Merz-Kollman-Singh method at the MP2/3-21G level. The standard deviations of the difference between electric charges obtained by both methods were 0.098 *e* and 0.079 *e* for  $[Cd(CN)_4]^{2-}$  and  $[Cd_2(CN)_7]^{3-}$ .
- (28) Iwamoto, T.; Nishikiori, S.; Kitazawa, T.; Yuge, H. *J. Chem. Soc., Dalton Trans.* **1997**, 4127.
- (29) (a) Reichardt, C. *Angew. Chem., Int. Ed. Engl.* **1965**, 4, 29. (b) Davis, K. M. C.; Symons, M. C. R. *J. Chem. Soc.* **1965**, 2709. (c) Offen, H. W.; Abidi, M. S. F. A. *J. Chem. Phys.* **1966**, 44, 4642. (d) Reichardt, C. *Chem. Soc. Rev.* **1992**, 21, 147.
- (30) Intensity data collection and structure analysis were carried out by the same methods used for the clathrate. Crystal data for  $[MV^{2+}][PF_6^-]_2 \cdot [C_6H_4(OCH_3)_2]_2 \cdot C_{20}H_{24}F_{12}N_2O_2P_2$ , *FW* = 614.35, monoclinic, space group *P2<sub>1</sub>/n* (no. 14), *a* = 7.3945(1) Å, *b* = 11.5399(2) Å, *c* = 30.4358(4) Å,  $\beta$  = 94.7525(6)°, *U* = 2588.21(7) Å<sup>3</sup>, *Z* = 4, *D<sub>x</sub>* = 1.58 g cm<sup>-3</sup>,  $\mu$ (Mo K $\alpha$ ) = 0.276 mm<sup>-1</sup>, 59 771 reflections measured, 7420 unique (*R<sub>int</sub>* = 0.042), *R1*(*F*) = 0.0670 for reflections with *I* > 2 $\sigma$ (*I*), *wR2*(*F*<sup>2</sup>) = 0.2277, *S* = 0.874 for all reflections and 343 parameters. The interplane distances between  $MV^{2+}$  and ODMB were 3.442(5) and 3.464(5) Å. Crystallographic data were deposited in the Cambridge Crystallographic Data Center as CCDC 207322.
- (31) (a) Kochi, J. K.; Rathore, R.; Maguerès, P. L. *J. Org. Chem.* **2000**, 65, 6826. (b) Maguerès, P. L.; Lindeman, S. V.; Kochi, J. K. *Org. Lett.* **2000**, 2, 3567. (c) Maguerès, P. L.; Lindeman, S. V.; Kochi, J. K. *J. Chem. Soc., Perkin Trans. 2*, **2001**, 1180. (d) Ganesan, V.; Rosokha, S. V.; Kochi, J. K. *J. Am. Chem. Soc.* **2003**, 125, 2559 and references therein.